Supplementary Figure

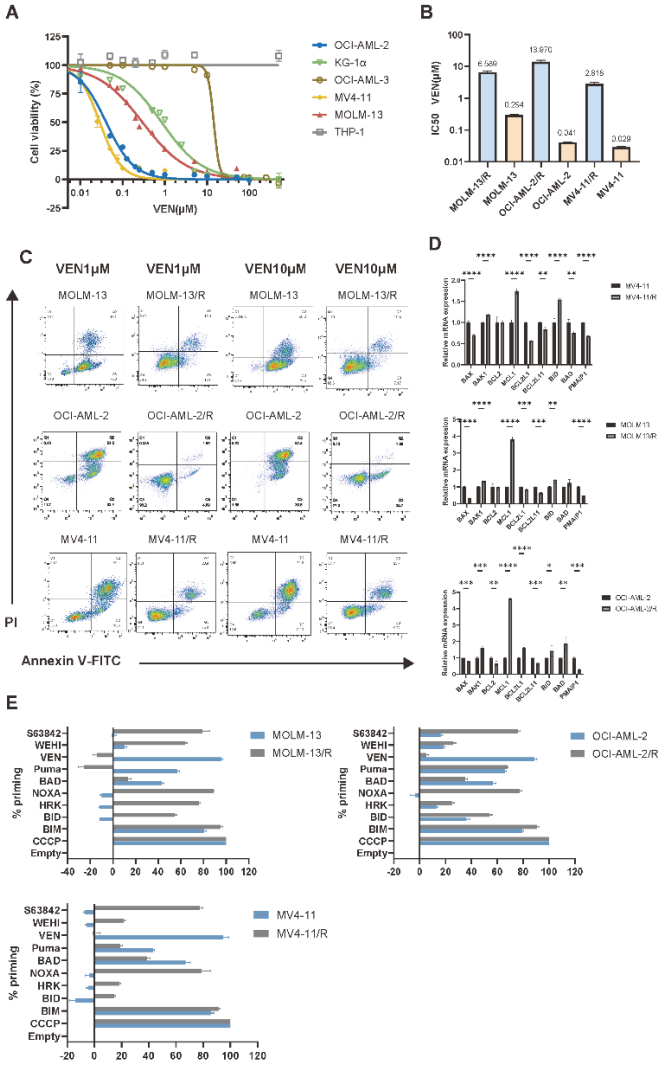

Figure S1. Generation and apoptotic characterization of venetoclax-resistant AML cell lines. **(A)** Dose-response curves of a panel of human AML cell lines treated with increasing concentrations of venetoclax (VEN) for 48 h. Cell viability was assessed by CCK-8 assay. Data represent mean ± SD (n = 3 independent experiments). **(B)** Comparison of VEN half-maximal inhibitory concentrations (IC_{50}) between parental and resistant (R) AML cell lines. IC_{50} values were calculated via non-linear regression analysis. Data are mean ± SD (n = 3). **(C)** Representative flow cytometric plots of Annexin V/PI staining in parental and VEN-resistant (R) AML cell lines following 48 h treatment with indicated doses of VEN. Quantification of apoptotic fractions is provided in the corresponding main figure. **(D)** Relative mRNA expression of BCL-2 family members in parental versus VEN-resistant (R) AML cell lines, determined by qRT-PCR. Expression levels were normalized to GAPDH. Statistical significance was determined by Student's t-test (*P < 0.05, **P < 0.01, ***P < 0.001, ****P < 0.0001). **(E)** BH3 profiling of mitochondrial priming in parental and VEN-resistant (R) AML cell lines. Mitochondrial depolarization (%) was measured by JC-1 assay following exposure to BH3-only peptides (10 μM) or small-molecule inhibitors (VEN, BCL-2i; S63845, MCL-1i; WEHI-539, BCL-XLi). CCCP and empty wells served as positive and negative controls, respectively (n = 1).

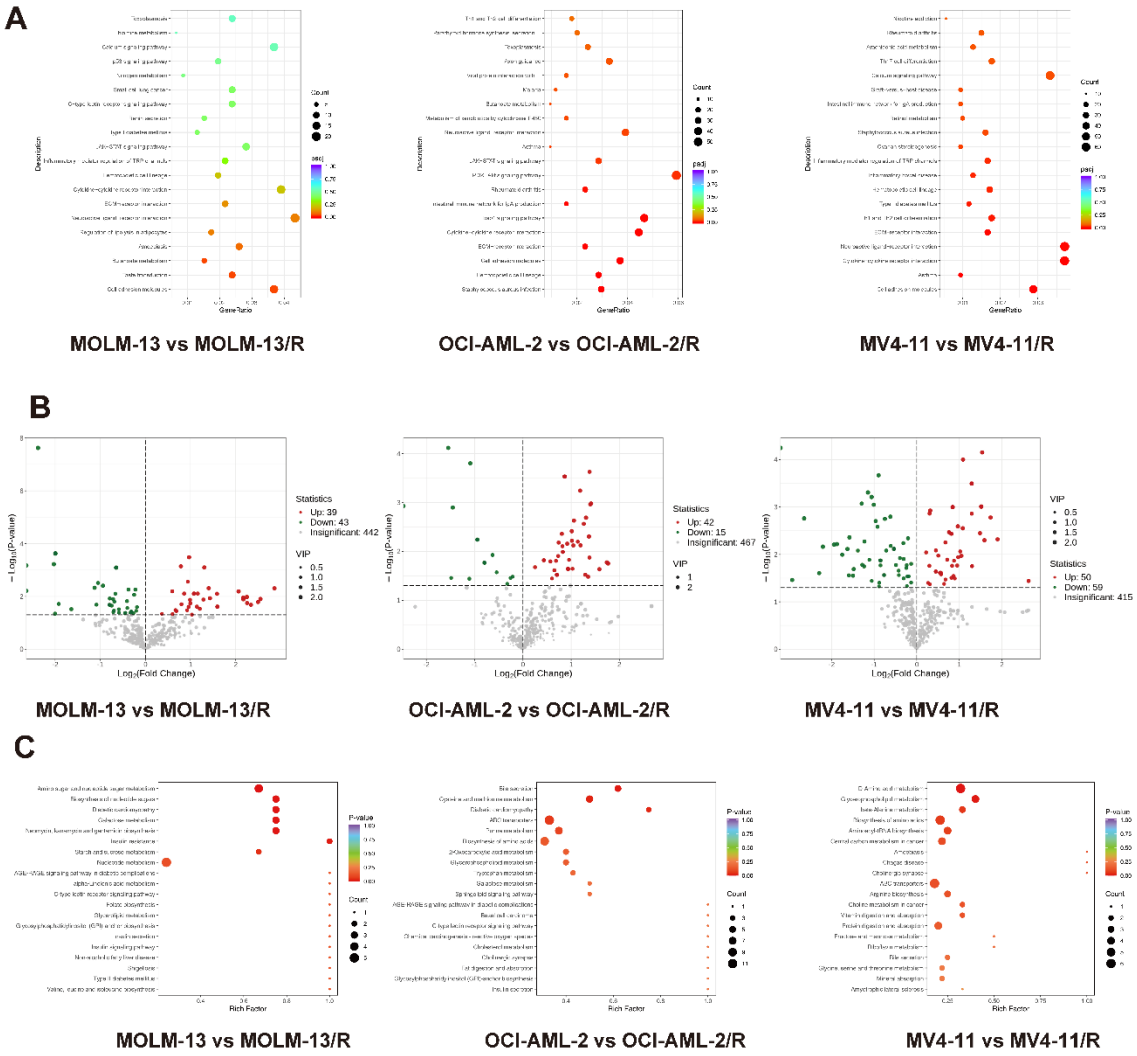

Figure S2. Integrated transcriptomic and metabolomic reprogramming in venetoclax-resistant AML cell lines.

(A) KEGG pathway enrichment analysis of differentially expressed genes (DEGs) between parental and venetoclax-resistant (R) AML cell lines (n = 3 biological replicates per group). DEGs were identified by RNA-seq using edgeR ($|\log_2FC| > 1$ and Padj < 0.05). The top 20 enriched pathways are ranked by Padj; dot size corresponds to gene count and color indicates the significance level. **(B)** Volcano plots illustrating differentially abundant metabolites in parental versus venetoclax-resistant (R) AML cell lines, identified via untargeted LC-MS/MS metabolomics (n = 6 biological replicates per group). Significantly upregulated (red) or downregulated (blue) metabolites were defined by VIP > 1 and $|\log_2FC| > 1$ derived from OPLS-DA modeling. Gray dots represent metabolites that did not meet significance thresholds. **(C)** KEGG metabolic pathway enrichment analysis of the differentially abundant metabolites identified in (B). The RichFactor denotes the ratio of differentially abundant metabolites to the total annotated metabolites within each pathway. Dot size represents metabolite count and color indicates the Padj.

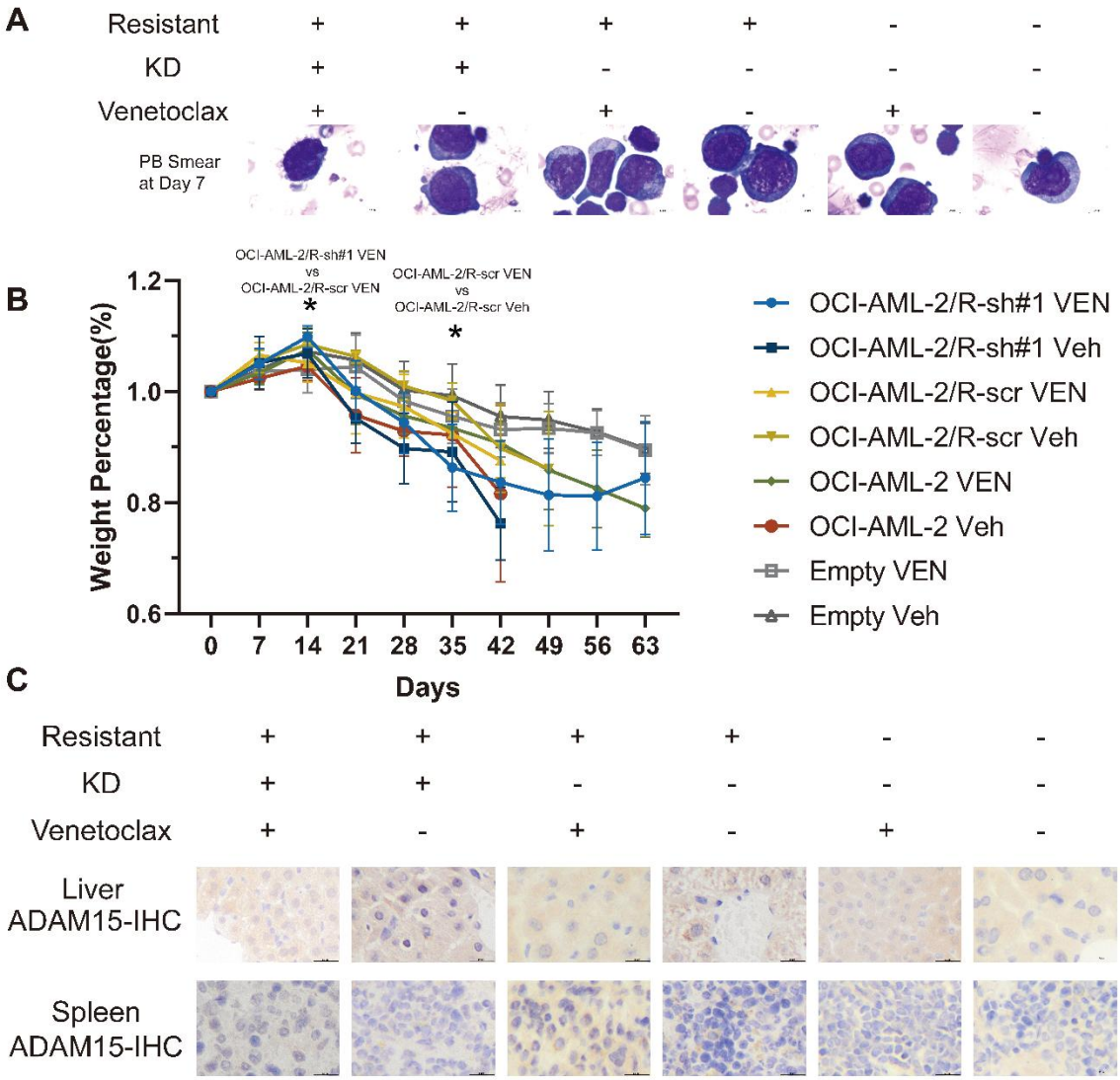

Figure S3. In vivo evaluation of ADAM15 knockdown and venetoclax efficacy in an OCI-AML-2 systemic xenograft model.

(A) Representative Wright-Giemsa-stained peripheral blood smears from NOD/SCID mice at day 7 post-transplantation. Mice were systemically engrafted via tail vein injection with parental OCI-AML-2 cells or their venetoclax-resistant (R) or ADAM15-knockdown (sh#1) derivatives. Smears illustrate the baseline peripheral blast burden and confirm successful leukemic engraftment prior to treatment initiation. **(B)** Longitudinal body weight monitoring of tumor-bearing and non-tumor-bearing (Empty) mice. Following engraftment confirmation on day 7, mice received daily oral gavage of venetoclax (VEN, 50 mg/kg) or vehicle (Veh). Data are presented as body weight percentage relative to day 0. Statistical significance was assessed by two-way ANOVA ($n \geq 6$ mice per group). Asterisks indicate significant differences between the indicated treatment cohorts (*$P < 0.05$). **(C)** Representative immunohistochemical (IHC) staining for ADAM15 in liver and spleen sections collected at the experimental endpoint. Images confirm the in vivo maintenance of ADAM15 knockdown within leukemic infiltrates and reveal differential ADAM15 expression between tumors derived from resistant and parental cells in these major organs. Scale bars, 50 µm.

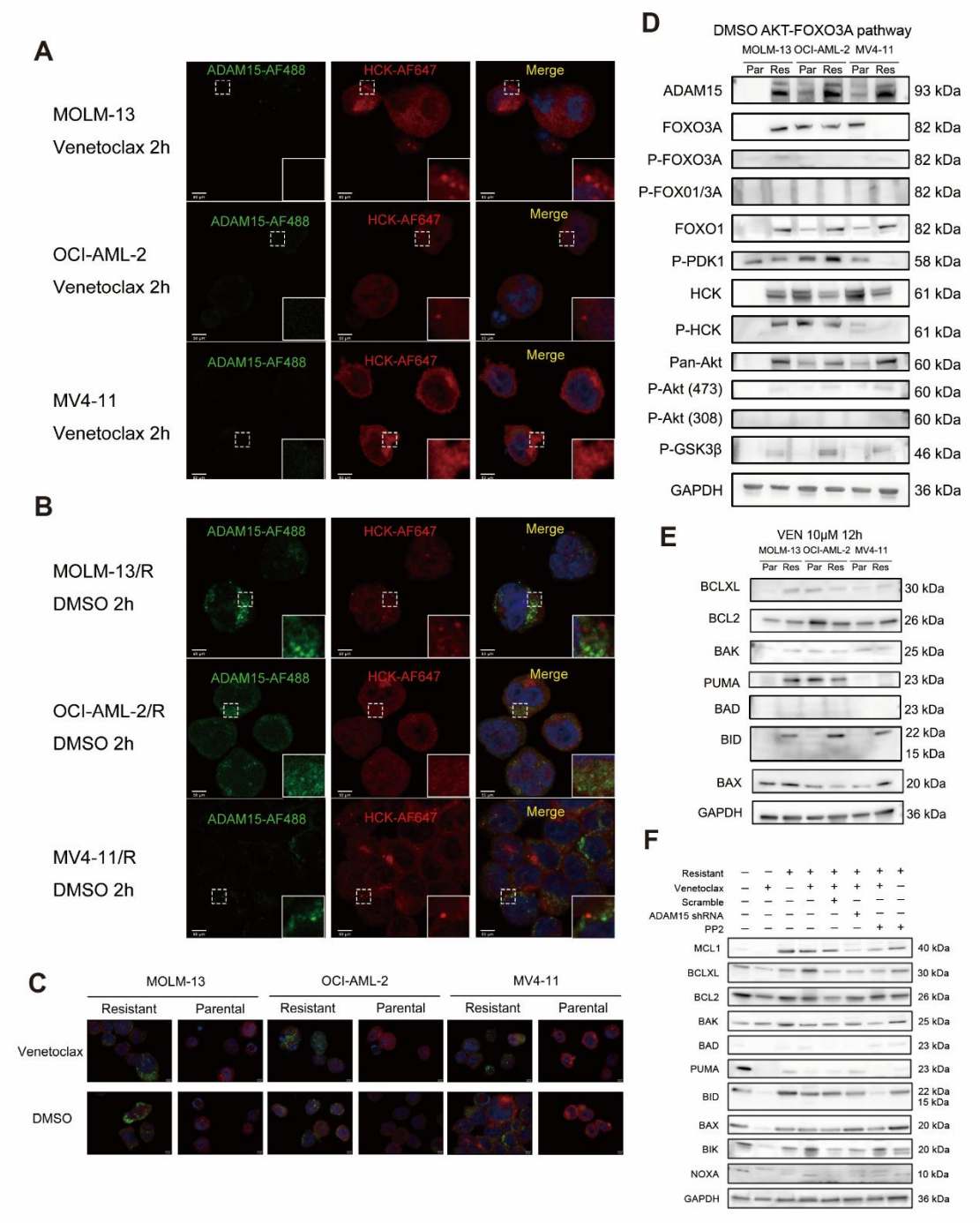

Figure S4. Characterization of the ADAM15–HCK interaction and downstream apoptotic signaling in Venetoclax-resistant AML cells.

(A, B) Representative confocal immunofluorescence images displaying the subcellular localization of ADAM15 (AF488, green) and HCK (AF647, red) in parental AML cell lines treated with 10 μM Venetoclax (VEN) for 2 hours **(A)**, and in VEN-resistant (/R) AML cell lines treated with a DMSO vehicle control for 2 hours **(B)**. Insets highlight magnified regions of interest. Scale bars, 50 μm. Images are representative of five distinct fields per condition across three independent experiments. **(C)** Merged immunofluorescence images illustrating the colocalization of ADAM15 and HCK across the three parental and VEN-resistant cell line pairs (MOLM-13, OCI-AML-2, and MV4-11) following a 2-hour treatment with 10 μM VEN or DMSO. Scale bars, 50 μm. Images are

representative of five fields per condition from three independent experiments. **(D)** Co-immunoprecipitation (Co-IP) assay demonstrating the endogenous physical interaction between ADAM15 and HCK in OCI-AML-2 cells treated with VEN for 2 hours. Isotype-matched immunoglobulins (Gt, goat; Rb, rabbit) served as negative controls for the immunoprecipitation. **(E)** Western blot analysis evaluating the basal expression and phosphorylation status of the ADAM15/HCK/AKT/FOXO3A signaling axis in parental (Par) and VEN-resistant (Res) AML cell lines under vehicle control (DMSO) conditions. GAPDH was utilized as a loading control. Representative blots from three independent experiments are shown. **(F)** Immunoblot profiling of pro- and anti-apoptotic BCL-2 family proteins in parental and VEN-resistant AML cell lines following treatment with 10 μM VEN for 12 hours. GAPDH served as a loading control. Representative blots from three independent experiments are shown. **(G)** Western blot analysis evaluating the expression of BCL-2 family proteins in VEN-resistant OCI-AML-2 cells under modified signaling conditions. Cells were subjected to either ADAM15 knockdown (ADAM15 shRNA) or pharmacological inhibition of HCK (PP2) in the presence (+) or absence (–) of VEN. A scramble shRNA served as a negative control. GAPDH was utilized as a loading control.